Quasiparticle Tunneling through a Barrier in the Fractional Quantum Hall Regime

Elad Shopen,[1] Yuval Gefen,[2] and Yigal Meir[1,3]

[1]*Department of Physics, Ben-Gurion University, Beer-Sheva 84105, Israel*
[2]*Department of Condensed Matter Physics, The Weizmann Institute of Science, Rehovot 76100, Israel*
[3]*The Ilse Katz Center for Meso- and Nano-Scale Science and Technology, Ben-Gurion University, Beer-Sheva 84105, Israel*

(Received 7 April 2005; published 22 September 2005)

Tunneling of fractionally charged quasiparticles (QPs) *through a barrier* is considered in the context of a multiply connected geometry. In this geometry global constraints do not prohibit such a tunneling process. The tunneling amplitude is evaluated and the crossover from mesoscopic QP-dominated to electron-dominated tunneling as the system's size is increased is found. The presence of disorder enhances both electron and QP-tunneling rates.

DOI: 10.1103/PhysRevLett.95.136803 PACS numbers: 73.43.−f, 73.23.−b

One of the most remarkable facts about the fractional quantum Hall effect (FQHE) is the existence of fractionally charged quasiparticles (QPs). Their dynamics is manifest in a host of physical phenomena, whose observation strongly supported the veracity of Laughlin's theory [1]. It has been pointed out [2,3] that QP tunneling is distinctly different from electron tunneling. Perturbative renormalization-group (RG) analysis [4] has indicated that in the weak backscattering limit interedge tunneling through the FQHE liquid is dominated by QP tunneling. These predictions have been confirmed by experiments [5]. In the opposite limit of strong backscattering (nearly disconnected FQHE systems coupled by weak tunneling through an insulator), the same RG analysis would have predicted that tunneling should be dominated again by QP tunneling. Common wisdom, however, has it that in this limit only electron tunneling is possible. The rationale for that goes as follows: consider two FQHE puddles weakly connected through tunneling. The total number of electrons on each puddle is (nearly) a good quantum number; hence it must be an integer. QP tunneling would render this number noninteger, and therefore such a process must be excluded.

Our starting point here is to note that there are setups where the above mentioned ''global constraint'' (i.e., the number of electrons on each side of the barrier being an integer) does not exclude *a priori* QP tunneling through a potential barrier. The common wisdom alluded to above needs then to be reexamined. Studying these setups is particularly interesting in view of recent experimental results which suggest the coexistence of both electron and QP tunneling under strong backscattering conditions [6], or cast doubt on the global constraint hypothesis [7].

Consider first the annulus depicted in Fig. 1(a). Clearly, the passage of a QP through the barrier would not violate the global constraint. There are two possible trajectories (for the presumed noiseless incoming current) to traverse the system: either following the edge adiabatically, or by tunneling through the barrier. The outgoing current would then be noisy [8]. By analyzing this nonequilibrium noise, one may detect the effective charge involved. Additionally, the charge of the tunneling QP may be reflected in the periodicity of the Aharonov-Bohm interference between the two paths.

Our extensive analysis, performed on a torus geometry described below, leads to three main results: (i) For our multiply connected geometry and in the presence of a real potential barrier we confirm the existence of QP tunneling, which decreases rapidly with system size [Eq. (3)]. (ii) We study the amplitude of such QP-tunneling processes and identify the crossover, in terms of the system's parameters, between the electron-tunneling-dominated and the QP-dominated regimes. (iii) We show that in FQHE systems, the presence of impurities may enhance both electron and QP-tunneling amplitudes [Eq. (5)], in the spirit of the Shklovskii-Li-Thouless mechanism [9].

The torus geometry.—To facilitate our analytical study and to avoid complications emanating from the system being open, we hereafter focus on a setup defined on a torus, spanned by the two periodic coordinates $0 < x < 2\pi R$ and $0 < y < L$ [Fig. 1(b)], with a uniform magnetic field perpendicular to the surface of the torus. On top of the torus surface we introduce a circular potential ridge (V_0). The tunneling investigated here is between the two sides of this barrier. The main steps in the analysis are as follows:

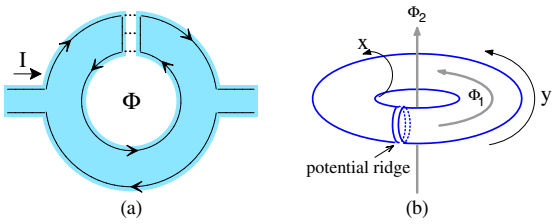

FIG. 1 (color online). (a) Proposed experimental setup for an annulus, allowing the tunneling of both QPs and electrons through a barrier. The edge states are marked. (b) The torus geometry studied in this work; x and y represent two Cartesian coordinates, the unit cell being $2\pi R \times L$; Φ_1 and Φ_2 are two Aharonov-Bohm fluxes threading the torus. A Hall liquid (of density $1/m$) covers the torus everywhere except around the barrier which is initially dry (''extended holes''). Here the barrier potential is circularly symmetric.

(i) We first construct modified Laughlin-Haldane-Rezayi states which correspond to a bulk filling factor $1/m$ (the "wet area") and a "dry area" (made of extended holes) where the electron density is suppressed, ideally to zero. The ground-state configuration is obtained by maximizing the overlap of the dry area of the many-body configuration with the barrier [10]. (ii) The Hamiltonian, and hence the wave functions, depends on two gauge fluxes, Φ_1 and Φ_2 [Fig. 1(b)]. By adiabatically increasing Φ_1 any many-body configuration will slide rigidly in the y direction, giving rise to a change in its energy. As the levels of two different configurations cross, the ground state of the system changes abruptly. Below we show that such a change corresponds to a tunneling event. The set of many-body energy levels is plotted in Fig. 2(a). (iii) To enable tunneling we break the circular symmetry (in the x direction), introducing an additional asymmetric potential (V_1). This gives rise to finite matrix elements between different configurations. Avoided-crossing gaps in the energy-flux spectrum [Fig. 2(a)] are a manifestation of tunneling: the period in flux reflects the nature of the particle that tunnels. Below we calculate these tunneling matrix elements. (iv) We demonstrate quantitatively how the presence of a multitude of δ-function impurities enhances the tunneling.

Our initial Hamiltonian is $H = H_0 + U_{\rm int} + V_0$, where H_0 includes the kinetic part as well as the magnetic field and fluxes and $U_{\rm int}$ is the two-particle interaction. The barrier potential V_0 is assumed to be sufficiently weak to exclude mixing with higher Landau levels.

For $V_0 = 0$ and no dry area, Haldane and Rezayi [11] have found a set of m degenerate Laughlin wave functions. The solution is obtained for a magnetic field which is quantized according to Dirac's condition $RL = \ell_H^2 N_\phi$, where N_ϕ is the number of magnetic flux quanta perpendicular to the torus surface and $\ell_H \equiv \sqrt{\hbar c/eB}$ is the magnetic length. These wave functions are eigenfunctions of total quasimomentum (TQM) [12] and, similarly to the Laughlin wave function [13], are exact (zero-energy) ground states of the Hamiltonian with hard-core interaction [i.e., $\nabla^2\delta(\vec{r})$]. Their ground-state electron density is nearly uniform. Here $N_\phi = mN$, where N is the number of electrons.

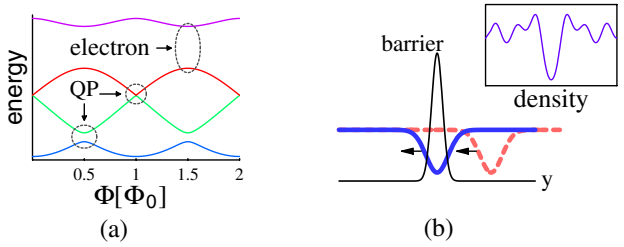

FIG. 2 (color online). (a) Intersecting energy curves as a function of the flux Φ_1. Avoided crossings correspond to tunneling of electrons and QPs as indicated. For QP (electron) tunneling the periodicity of the adiabatically varied ground-state energy is ϕ_0 ($3\phi_0$) [3]. (b) Schematic density profile of the initial ground state Ψ_0 (solid line) and the first excited state Ψ_1 (dashed line). As Φ_1 increases, these density profiles slide to the left, Ψ_1 eventually becomes the ground state. Inset: An actual density profile for $m = 3$, $N = 6$, and $N_h = 1$. Densities corresponding to other wave functions are rigid shifts thereof.

Extended hole wave functions.—To render the barrier (and its close vicinity) "dry," we tune the magnetic field to allow for N_h holes: $N_\phi = mN + N_h$. The lowest Landau level consists of N_ϕ single-particle states $|n\rangle$ (cf. Ref. [11]). The density profile of each single-particle state is approximately a Gaussian in the y direction and uniform in the x direction. The distance between the guiding centers of adjacent states is L/N_ϕ. In the subspace of the lowest Landau level [spanned by $\binom{N_\phi}{N}$ possible Slater Determinants] the ground state is determined solely by the interaction. Diagonalizing the hard-core interaction results in a set of zero-energy ground states, each having N_h holes extended in the x direction. As an example, consider $N_h = 1$. When the interaction term is diagonalized, one obtains N_ϕ Laughlin-like states of zero energy. Each of these states corresponds to a nonuniform electron density: the filling is $1/m$ almost everywhere, but the occupation of one of the single-particle quasimomentum states $|n\rangle$ is suppressed: the area around this guiding center is dry [Fig. 2(b)]. We denote such a many-body state with an extended hole at $|n\rangle$ by Ψ_n [14]. It is an eigenstate of the TQM. By sliding all guiding centers rigidly by 1 we increase the TQM by N, shifting $\Psi_n \to \Psi_{n+1}$. The above procedure is readily generalized to $N_h > 1$. Choosing the N_h holes to be contiguous leads to a dry area of a desired width [15].

Tunneling: Electrons versus QPs.—The initial ground state whose dry area coincides with the barrier is denoted by Ψ_0. As the flux Φ_1 is varied adiabatically this many-body configuration slides rigidly around the torus. The dry area of Ψ_0 moves and its energy $E_0(\Phi_1)$ increases. The dry area of Ψ_1, whose TQM differs from that of Ψ_0 by $N \bmod(N_\phi)$, slides towards the barrier and its energy $E_1(\Phi_1)$ decreases. When Φ_1 is increased by $\phi_0/2$, $E_0(\Phi_1)$ and $E_1(\Phi_1)$ intersect, and the ground state of the system switches $\Psi_0 \to \Psi_1$. This corresponds to a shift of each single electron state by 1: $|n\rangle \to |n+1\rangle$. Since the average occupation of $|n\rangle$ is $1/m$, this process describes a shift of charge of e/m from one side of the barrier to the other, i.e., QP tunneling. The level-crossing degeneracy is lifted by breaking the circular symmetry of the potential V_0: $H \to H + V_1$. The QP-tunneling matrix element is $\langle\Psi_0|V_1|\Psi_1\rangle$. By analogy, the two many-body states Ψ_0 and Ψ_m differing in their TQM by $mN \bmod(N_\phi)$ will cross when Φ_1 increases by $m\phi_0/2$; hence $\langle\Psi_0|V_1|\Psi_m\rangle$ is the matrix element for electron tunneling. In order to evaluate these tunneling matrix elements, we use the fact that V_1 is a single-particle potential. The overlap $\langle\Psi_0|V_1|\Psi_p\rangle$ ($p = 1, m$ for QP and electron tunneling, respectively) consists of contributions from the respective Slater determinants components $|k_1, \ldots, k_N\rangle \in \Psi_0$ and $|\ell_1, \ldots, \ell_N\rangle \in \Psi_p$, which are identical except for a single pair $\tilde{k}, \tilde{\ell}$. The

difference in TQM is

$$\tilde{\ell} - \tilde{k} = pN \bmod(N_\phi). \quad (1)$$

Taking $V_1 = \tilde{V}_1 \delta(x)$ renders the procedure particularly simple [16]. Then $\langle \tilde{k}|V_1|\tilde{\ell}\rangle \equiv v_p$ depends only on the difference $\tilde{\ell} - \tilde{k}$. The tunneling amplitude can then be cast as $\mathcal{T}_p \equiv \langle \Psi_0|V_1|\Psi_p\rangle = \mathbf{f}_p(L)\mathbf{v}_p$, where $\mathbf{f}_p$ is a combinatorial factor resulting from summation over all possible pairs satisfying (1) and is calculated numerically. For $\mathbf{v}_p$ one readily obtains

$$\mathbf{v}_p = \frac{\tilde{V}_1}{R} \sum_{q=-\infty}^{\infty} e^{-iq\Phi_2} \exp\left\{-\left[(p - qN_\phi)\frac{L}{2N_\phi \ell_H}\right]^2\right\}. \quad (2)$$

To leading order $\mathbf{v}_p \propto \exp[-(pN \bmod N_\phi \frac{L}{2N_\phi \ell_H})^2]$. This reflects the overlap of two Gaussians separated by a distance pNL/N_ϕ on the torus [Fig. 3(a)]. For a QP the separation is of the order L/m ($N_\phi = mN + N_h$), so $\mathbf{v}_p$ scales as $\exp[-(L/2m\ell_H)^2]$. By contrast, for electrons the separation distance (defined modulo L) is $N_h L/N_\phi$; hence $\mathbf{v}_p$ scales as $\exp[-(LN_h/2N_\phi \ell_H)^2] = \exp[-(N_h \ell_H/R)^2]$, which is L independent (where we used the Dirac condition). Likewise we find that the factor $\mathbf{f}_p$ is roughly system-size independent for electron tunneling, while it rapidly decreases (Gaussian-like) for QPs.

We thus summarize

$$\mathcal{T}_p \sim \begin{cases} e^{-\alpha L^2/\ell_H^2}, & \text{QPs } (p=1) \\ L \text{ independant}, & \text{electrons } (p=3) \end{cases}. \quad (3)$$

For $N_h = 1$ (and $N = 2, \ldots, 6$) we obtain numerically $\alpha \approx 0.07$ [Fig. 3(b)]. We expect this to approach $1/12 (= 1/4m)$ in the thermodynamic limit [cf. Eq. (5) for $N_{\rm imp} = 1$]. Note that the factor $\mathbf{f}_{p=1}$ further suppresses the single-particle term $e^{-(L/2m\ell_H)^2} \to e^{-(L/2\ell_H)^2/m}$.

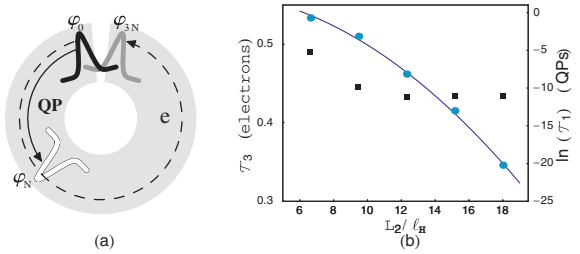

FIG. 3 (color online). Tunneling involves initial and final states whose TQM differ by pN, $p = 1, 3$ for QPs and electrons, respectively. Here $m = 3$. The respective matrix elements involve the overlap of two single-particle states (Gaussians), whose separation is pNL/N_ϕ. For QPs the latter is of the order of L/m (solid arrow, black and white Gaussians). Thus the overlap factor for QPs, $v_{p=1}$, strongly decreases with L. By contrast, for electrons (dashed arrow, black and gray) the distance (defined modulo L) is $N_h L/N_\phi \ll L$ and the dependence on L is negligible. (b) The calculated tunneling probabilities for electrons ($\mathcal{T}_3$) and QPs ($\mathcal{T}_1$), for $m = 3$, $N_h = 1$. $\mathcal{T}_3$ is practically independent of system size (squares), while for QPs $\mathcal{T}_1 \sim e^{-\alpha L_2^2/\ell_H^2}$ (circles). The solid line is a fit with $\alpha \approx 0.07$.

Impurity-assisted tunneling.—We next introduce impurities into the system, $\mathcal{H} = H_0 + U_{\rm int} + V_2$, where $V_2 \equiv \sum_{j=1}^{N_{\rm imp}} V_{\rm imp}\delta(z - z_{0j})$ represents $N_{\rm imp}$ localized impurities ($V_{\rm imp} > 0$). Shklovskii, Li, and Thouless [9] have shown that, for noninteracting electrons, impurities modify the Gaussian decay of the edge-to-edge Green function into exponential. This result is generalized here to the fractional quantum Hall regime. To simplify the analysis we employ the fact that QP tunneling may be interpreted as a nonlocal process taking place through the liquid, while electron tunneling takes place through both the potential barrier and the liquid. Thus, the torus can be effectively replaced by two cylinders whose circumference is $2\pi R$ and whose lengths are $L_{\rm barrier} \equiv N_h L/N_\phi$ and $L_{\rm liquid} \equiv L - L_{\rm barrier} = mNL/N_\phi$. For a cylinder with impurities the ground-state wave function $\Psi_{\{\mathbf{z}_0\}}$ contains $N_{\rm imp}$ localized holes at the impurity positions

$$\Psi_{\{\mathbf{z}_0\}} = \prod_{j=1}^{N_h}\prod_{k=1}^{N}(e^{-iz_k/R} - e^{-iz_{0j}/R})\Psi_L \quad (4)$$

[$\Psi_L = \prod_{i<j}(e^{-iz_i/R} - e^{-iz_j/R})^m e^{-\Sigma_j y_j^2/2}$ is Laughlin's cylinder wave function].

To obtain the various tunneling matrix elements, we calculate the overlap between $\Psi_{\{\mathbf{z}_0\}}$ and its shifted version $\tilde{\Psi}_{\{\mathbf{z}_0\}} = \prod_{j=1}^{N} e^{-ipz_j/R}\Psi_{\{\mathbf{z}_0\}}$, $p = 1, m$ for QP and electron tunneling, respectively. For $N_{\rm imp} = 1$ one recovers (up to prefactors) the perturbative result [17]: QPs tunnel more efficiently than electrons along a cylinder. We have evaluated this overlap numerically for systems with $N \le 6$ (for electrons tunneling at integer filling, we have considered $N \le 17$) and $N_{\rm imp} \le 4$, for (i) impurities equally spaced on a line and (ii) at random positions throughout the cylinder, averaging over $\sim$1000 realizations. For case (i) we find that

$$\langle \Psi_{\{\mathbf{z}_0\}}|\tilde{\Psi}_{\{\mathbf{z}_0\}}\rangle \sim \begin{cases} e^{-L^2/12N_{\rm imp}\ell_H^2}, & \text{QPs} \\ e^{-L^2/4N_{\rm imp}\ell_H^2}, & \text{electrons} \end{cases} \quad (5)$$

agrees with the numerics. For case (ii) the decay factor of the exponent is modified, but not the parametric dependence. We find that when the longitudinal impurity density $\lambda = L/N_{\rm imp}$ is held constant, the typical hopping distance is kept fixed, a Gaussian-to-exponential crossover takes place. This crossover can be understood in terms of multiple impurity-assisted tunneling. For a QP, as an example, $e^{-L^2/12N_{\rm imp}} \to e^{-\lambda L/12}$.

QP-electron crossover.—Studying this crossover is now experimentally feasible [18]. Here we present a framework to study it theoretically in a multiply connected geometry, e.g., the torus. As $L_{\rm barrier}$ is varied (compared with $L_{\rm liquid}$) the QP tunneling $\mathcal{T}_1$ competes with the electron tunneling $\mathcal{T}_3$. By calculating $\mathcal{T}_1$ and $\mathcal{T}_p$, as explained above, varying the number of particles (modification of $L_{\rm liquid}$) and the number of extended holes (modification of $L_{\rm barrier}$),

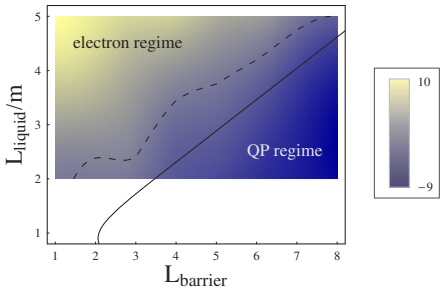

FIG. 4 (color online). Electron-QP crossover: Plotted is the interpolation of $\ln(\mathcal{T}_3/\mathcal{T}_1)$ for discrete values of N and N_h corresponding to $L_{\rm liquid}/m$ and $L_{\rm barrier}$, respectively (measured in units of ℓ_H^2/R; here $R = \sqrt{14\pi}$). Dashed line: the crossover curve $\mathcal{T}_3 = \mathcal{T}_1$. Solid line: an approximated crossover curve obtained by taking $e^{-L_{\rm liquid}^2/12\ell_H^2} = e^{-L_{\rm barrier}^2/4\ell_H^2} + e^{-L_{\rm liquid}^2/4\ell_H^2}$.

we obtain the ratio of the electron-tunneling amplitude to that of QP tunneling (Fig. 4). This allows us to determine the separation between the electron-tunneling dominated and the QP-tunneling dominated regimes (dotted line). This can be compared to the solid curve obtained by taking the estimates $\mathcal{T}_1 \sim e^{-L_{\rm liquid}^2/4m\ell_H^2}$ and $\mathcal{T}_3 \sim e^{-L_{\rm barrier}^2/4\ell_H^2} + e^{-L_{\rm liquid}^2/4\ell_H^2}$.

Discussion.—By keeping the barrier size fixed and increasing the torus length, we have found that the QP-tunneling amplitude decreases while the electron amplitude is mostly unaffected. This supports the picture that the QP tunneling through a barrier [19], while in principle possible, is a mesoscopic effect. It may be interpreted as a QP leaping through the liquid around the barrier. In the thermodynamic limit the QP-tunneling amplitude vanishes, in accordance with common wisdom. The dependence of the tunneling amplitude on length scales does not conform to the scaling resulting from the RG treatment [4]. It is strongly modified by the multiple connectedness of the system. Adding disorder enhances the tunneling amplitudes. As can be seen from Eq. (5), special arrangements of the impurities can lead to even stronger enhancement (e.g., increase the linear density of $N_{\rm imp}$, while keeping the two-dimensional density fixed). We believe that the best candidate to test the ideas outlined here is the annulus geometry [Fig. 1(a)]. The relevance of the current results to the annulus geometry will be explored in future studies.

We thank A. Altland, F. D. M. Haldane, B. Halperin, B. I. Shklovskii, and D. J. Thouless for illuminating discussions on various aspects of the problem. This work was supported by the U.S.-Israel Binational Science Foundation, the Israel Academy of Science, and the Minerva Foundation. Y. G. was supported by the AvH foundation. Y. M. was supported through the Einstein Minerva Center for Theoretical Physics (through the BMBF).

[1] R. B. Laughlin, Phys. Rev. Lett. **50**, 1395 (1983).
[2] S. A. Kivelson and V. L. Pokrovsky, Phys. Rev. B **40**, R1373 (1989); S. Kivelson, Phys. Rev. Lett. **65**, 3369 (1990); J. A. Simmons, H. P. Wei, L. W. Engel, D. C. Tsui, and M. Shayegan, Phys. Rev. Lett. **63**, 1731 (1989); J. A. Simmons, S. W. Hwang, D. C. Tsui, H. P. Wei, L. W. Engel, and M. Shayegan, Phys. Rev. B **44**, 12 933 (1991); V. J. Goldman and B. Su, Science **267**, 1010 (1995).
[3] D. J. Thouless and Y. Gefen, Phys. Rev. Lett. **66**, 806 (1991); Y. Gefen and D. J. Thouless, Phys. Rev. B **47**, 10 423 (1993); see also Y. Avron, R. Seiler, and B. Shapiro, Nucl. Phys. **B265**, 364 (1986); D. J. Thouless, Phys. Rev. B **40**, R12034 (1989).
[4] K. Moon, H. Yi, C. L. Kane, S. M. Girvin, and M. P. A. Fisher, Phys. Rev. Lett. **71**, 4381 (1993); M. P. A. Fisher and L. I. Glazman, *Mesoscopic Electron Transport*, edited by L. Kowenhoven, G. Schoen, and L. Sohn, NATO ASI Series Vol. 345 (Dordrecht, Boston, 1997), p. 331.
[5] R. de-Picciotto, M. Reznikov, M. Heiblum, V. Umansky, G. Bunin, and D. Mahalu, Nature (London) **389**, 162 (1997); L. Saminadayar, D. C. Glattli, Y. Jin, and B. Etienne, Phys. Rev. Lett. **79**, 2526 (1997).
[6] E. Comforti, Y. C. Chung, M. Heiblum, and V. Umansky, Nature (London) **416**, 515 (2002); Y. C. Chung, M. Heiblum, and V. Umansky, Phys. Rev. Lett. **91**, 216804 (2003).
[7] J. Martin, S. Ilani, B. Verdene, J. Smet, V. Umansky, D. Mahalu, D. Schuh, G. Abstreiter, and A. Yacoby, Science **305**, 980 (2004).
[8] Note that only forward scattering is involved here. This means that the transmission probability is 1, implying the absence of noise in the dc limit. The noise alluded to above may be detected at finite frequencies.
[9] B. I. Shklovskii, Pis'ma Zh. Eksp. Teor. Fiz. **36**, 43 (1982) [JETP Lett. **36**, 51 (1982)]; Q. Li and D. J. Thouless, Phys. Rev. B **40**, 9738 (1989).
[10] For a ridge whose extension in the y direction is $L_{\rm barrier}$, the number of extended holes required to render the ridge dry is $N_h = [RL_{\rm barrier}/\ell_H^2] + 1$.
[11] F. D. M. Haldane and E. H. Rezayi, Phys. Rev. B **31**, R2529 (1985).
[12] The total angular momentum is defined mod(N_ϕ).
[13] F. D. M. Haldane, Phys. Rev. Lett. **51**, 605 (1983); S. A. Trugman and S. Kivelson, Phys. Rev. B **31**, 5280 (1985).
[14] In the present Letter we employ a numerical recipe for the construction of extended hole states. We note that these may also be obtained analytically, starting with Laughlin's state with localized holes. As this requires some detail, and is not crucial to understanding the present analysis, we will present it elsewhere. For $N_h = 1$: $\Psi_n = \int g_n^*(z_0)\Psi_{(z_0)}dz_0$, where g_n's are single-particle states on the *extended* unit cell $2\pi mR \times mL$, and $\Psi_{(z_0)}$ is a Laughlin state with a localized hole at z_0 [11].
[15] The width of a single-particle quasimomentum state in the y direction is ℓ_H. When $N_h < R/\ell_H$, we have a reduced density rather than a dry area.
[16] Other forms for V_1 lead to similar results.
[17] A. Auerbach, Phys. Rev. Lett. **80**, 817 (1998).
[18] E. Comforti, Y. C. Chung, M. Heiblum, and V. Umansky, Phys. Rev. Lett. **89**, 066803 (2002).
[19] The work of Helias and Pfannkuche (condmat/0403126) also supports the notion of QP tunneling through a barrier.